JACS
JOURNAL OF THE AMERICAN CHEMICAL SOCIETY

Communication

pubs.acs.org/JACS

On-Surface Solvent-Free Crystal-to-Co-crystal Conversion by Non-Covalent Interactions

Meital Boterashvili,[†] Michal Lahav,[†] Sreejith Shankar,[†] Antonio Facchetti,[‡] and Milko E. van der Boom*[,†]

[†]Department of Organic Chemistry, The Weizmann Institute of Science, 234 Herzl St., Rehovot 7610001, Israel

[‡]Department of Chemistry and the Materials Research Center, Northwestern University, 2145 Sheridan Road, Evanston, Illinois 60208, United States

Supporting Information

ABSTRACT: Enabling and understanding new methodologies to fabricate molecular assemblies driven by intermolecular interactions is fundamental in chemistry. Such forces can be used to control crystal growth and enable surface-confinement of these materials, which remains challenging. Here we demonstrate for the first time, a solvent-free on-surface crystal-to-co-crystal conversion process driven by halogen bonding (XB). By exposing a polycrystalline organic material, consisting of a XB-acceptor moiety, to the vapors of a complementary XB-donor compound, the corresponding halogen-bonded co-crystals were formed. Furthermore, we demonstrate that this approach can also be utilized for non-crystalline materials to afford surface-confined organic composites. Our stepwise vapor-based approach offers a new strategy for the formation of hybrid supramolecular materials.

Co-crystals are molecule-based solids consisting of at least two different molecular components held together by intermolecular forces. Such crystals are commonly formed from a solution containing both components.[1] Molecule-based crystal-to-crystal conversions might offer also a route toward the formation of co-crystals.[2] Despite recent advances in crystal engineering,[3] co-crystallization on solid surfaces remains challenging using known methodologies, and it would be desirable to realize new ones.[4] The control over the formation of polycrystalline thin films has been shown to be a key step for the formation of device-quality materials.[5] Such hybrid solids can possess improved or significantly different properties compared to those of the single-component systems.[6,7] A common strategy for co-crystal synthesis involves a one-pot approach in which a mixture of both compounds is loaded onto the surface, and co-crystallization occurs through slow solvent evaporation or spin coating.[4,8−10] This approach is lengthy and requires good solubility of both molecular components in the same solvent(s). Undesired formation of solvates is another drawback of growing crystals from solution. In addition, changes in thin-film crystallinity are usually induced thermally after film deposition.[11] Moreover, the formation of co-crystals using a solvent-free strategy would offer the possibility of polymorphic modifications of a material.[12] Herein we report the on-surface crystal-to-co-crystal conversion of a polycrystalline organic material. This transformation is driven by halogen bonding (XB).

Evidence for XB has been shown decades ago by Hassel and Schmidt.[13,14] In recent years, this donor−acceptor type of interaction between an electrophilic halogen atom (XB donor) and an electron donor (XB acceptor) has emerged as a potent non-covalent force in supramolecular chemistry.[15] Recent reports include advances in biomedical research,[16,17] functional organic-based materials,[7,18,19] and crystal engineering.[2a,20−22] In materials chemistry, a variety of functional XB-based materials were obtained, including co-crystals with tunable optical properties,[7,18] dynamic co-crystals,[2a] and photoresponsive liquid crystals.[23] Furthermore, XB has been shown to promote the formation of supramolecular assemblies on surfaces.[8,24−26] Our two-step solvent-free process for the formation of polycrystalline organic material involves consecutive physical vapor deposition (PVD) of the XB-acceptor, 1,4-bis((*E*)-2-(pyridin-4-yl)vinyl)benzene (**1**) and the XB-donor sym-triiodotrifluorobenzene ($C_6F_3I_3$; **2**). Exposure of polycrystalline organic films (**S1**) to vapors of compound **2** results in crystal-to-co-crystal conversion (**S1-2**, Figure 1). Co-crystallization of compounds **1** and **2** from solution resulted in the formation of an XB network consisting of N···I bonds.[22] Compound **2** was found to form two halogen bonds with **1** resulting in a co-crystal with a molar ratio of 1:1. Compound **1** undergoes efficient sublimation, as judged by thermogravimetric analysis (TGA; Figure S1), displaying the volatility and thermal robustness that are required for vacuum PVD. This method has been shown to be effective in forming crystalline organic-based films.[24] Compound **2** is sufficiently volatile at ambient pressure rendering vacuum PVD unnecessary for its evaporation. The **S1** films deposited on silicon and quartz substrates were characterized by UV/vis spectroscopy, atomic force microscopy (AFM), reversed-phase high-performance liquid chromatography (RP-HPLC), and X-ray diffraction (XRD).

The growth of **S1** was monitored with a quartz crystal microbalance (QCM) and indicated a film thickness of 20 nm. UV/vis spectroscopy measurements of **S1** showed an absorbance maximum at λ_{max} = 349 nm, correlating well with the absorbance maximum observed for compound **1** in solution (Figure S2a). The broadening of the absorbance band of **S1**, compared to that of compound **1** in solution, is attributed to the lack of solvent and/or packing interactions.[27] AFM measurements on silicon substrates revealed the formation of a homogeneous film consisting of elongated grains (mean

Received: July 9, 2014
Published: August 4, 2014

   dx.doi.org/10.1021/ja5066587 | *J. Am. Chem. Soc.* 2014, 136, 11926−11929

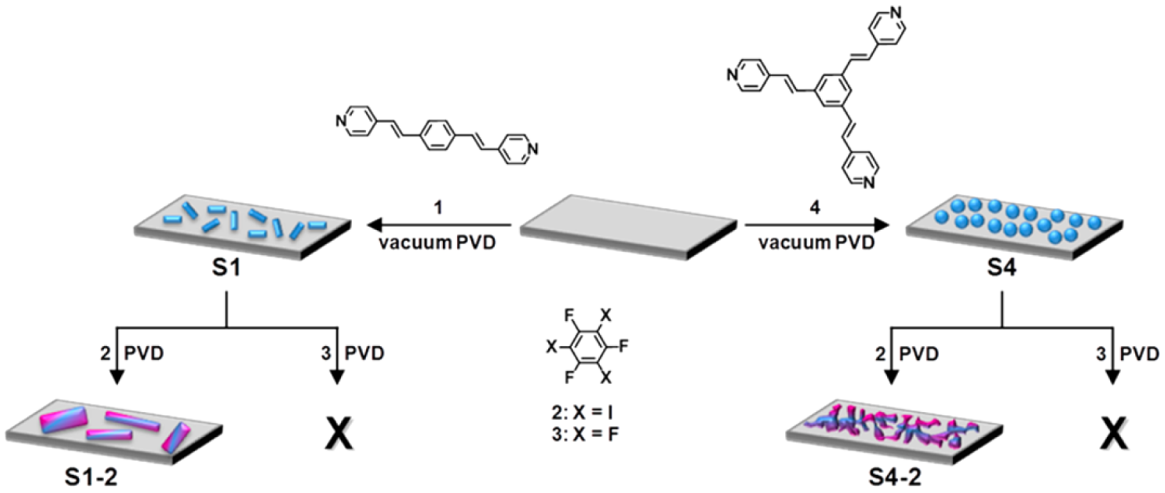

Figure 1. Crystal-to-co-crystal conversion by consecutive vapor-based deposition. The **S1** and **S4** interfaces are formed on silicon and quartz substrates by vacuum PVD of compound **1** or **4** (XB acceptors), respectively. Exposure of the polycrystalline **S1** surface to vapors (ambient pressure PVD) of compound **2** (XB donor) results in the formation of the corresponding surface-confined co-crystals **S1-2**. Exposure of the non-polycrystalline **S4** to vapors (ambient pressure PVD) of compound **2** results in the formation of the hybrid interface **S4-2**.

height = 60 ± 6 nm; surface coverage = 57%; Figures 2a and S3a,b). This height is different than the thickness observed by

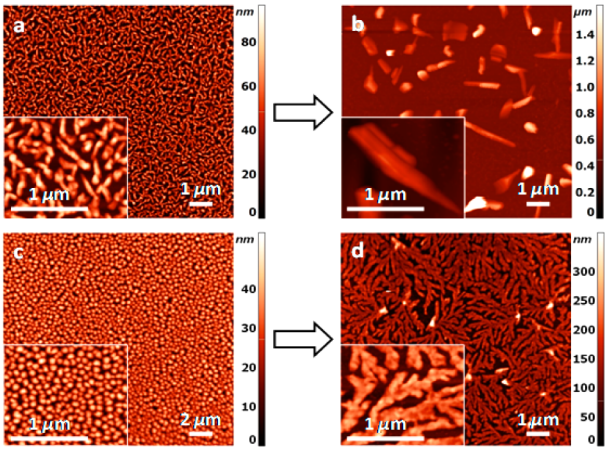

Figure 2. Representative AFM topography images of **S1**, **S1-2**, **S4**, and **S4-2** on silicon substrates. (a) 20 nm-thick **S1** obtained by vacuum PVD of compound **1**. (b) **S1-2** obtained by exposure of **S1** to vapors of compound **2** at 120 °C for 18 h. (c) 20 nm-thick **S4** obtained by vacuum PVD of compound **4**. (d) **S4-2** obtained by exposure of **S4** to vapors of compound **2** at 120 °C for 18 h. The insets are high-magnification images of the corresponding surfaces. For the inset AFM color palettes, see Figures S3 and S17.

the QCM. The AFM is a direct measurement of the morphology, whereas the QCM is weighing the total mass of the deposited material regardless of its morphology and translates it to the apparent thickness, assuming a continues film. The diffraction pattern obtained for **S1** correlates well with the main intensity powder diffraction signals of compound **1** (Figure 3a,c). This correlation demonstrates the polycrystalline nature of **S1**. Increasing the thickness of **S1** (from 20 to 50 nm measured by QCM) resulted in higher optical absorbance intensity (2.3 times higher) of the resulting surface (Figure S4). AFM images revealed denser films while retaining the overall grain morphology (Figure S5a,b). XRD analysis of these thicker assemblies revealed increased intensity of the diffraction peaks with increasing the thickness of **S1**, suggesting that the

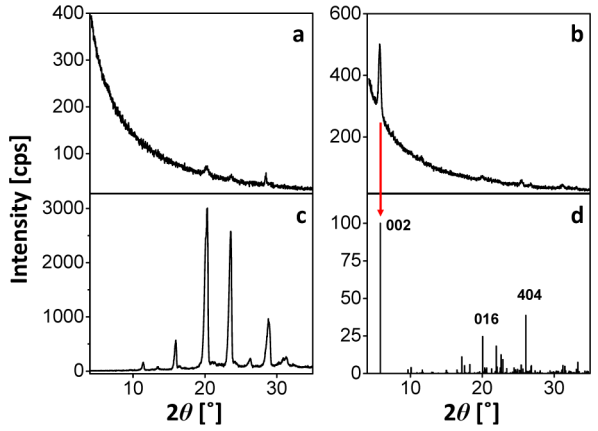

Figure 3. XRD analysis demonstrating the crystalline nature of **S1** and **S1-2**. (a,b) XRD patterns of 20 nm-thick **S1** and **S1-2**, respectively. (c) Powder XRD pattern of compound **1**. The absence of some reflections in (a), compared to the powder pattern in (c), is due to the relatively small amount of material on the surface. (d) Simulated XRD pattern of the corresponding co-crystal **1·2** grown from solution. The simulated pattern was obtained from the single crystal structure reported for the **1·2** co-crystal, using Jade 9.5 software. The XRD measurements of **S1** and **S1-2** were performed in the asymmetric 2θ scan mode. Powder XRD measurements were performed in the $\theta/2\theta$ scan mode.

structural order is retained throughout the deposition process (Figure S6).[24]

S1-2 was formed by exposing the 20 nm-thick **S1** to vapors of compound **2** (120 °C, 18 h), and its formation was confirmed by significant changes in the optical absorption spectrum, surface morphology, crystallinity, and molecular composition of the films. UV/vis spectroscopy of **S1-2** showed a significant broadening and red shift ($\Delta\lambda_{max} \approx 40$ nm) of the corresponding absorbance band compared to **S1** (Figure S4a).

AFM images of **S1-2** revealed a striking difference in morphology compared to **S1**, displaying non-uniform grains (Figures 2b and S3c,d). Field-desorption mass spectrometry (FD-MS) and reverse-phase high-performance liquid chromatography (RP-HPLC) analysis of redissolved **S1-2** confirmed the formation of a new composite consisting of both compounds **1** and **2** in a 1:1 molar ratio (Table S1, and

dx.doi.org/10.1021/ja5066587 | J. Am. Chem. Soc. 2014, 136, 11926−11929

Figures 4 and S7). Co-crystals **1·2** grown from solution were redissolved in ACN:H_2O (v/v = 1:1) and also analyzed by RP-HPLC. Interestingly, the RP-HPLC chromatograms for **S1-2** and the co-crystal **1·2** grown from solution are nearly identical (Figure 4b,c).[22] **S1-2** exhibits a different XRD pattern compared to that of **S1**, corroborating the change in film composition and suggesting the formation of a new crystalline structure (Figure 3a,b). Comparing the data obtained for **S1-2** with the simulated pattern for co-crystal **1·2** (grown from solution) revealed a clear correlation between the dominant diffraction signal observed at 2θ = 5.75° (d = 15.42 Å, hkl = 002) and the highest intensity diffraction signal expected for the co-crystal (Figure 3b,d). This signal was not obtained for either compound **1** or **2** independently (Figures 3c and S9).

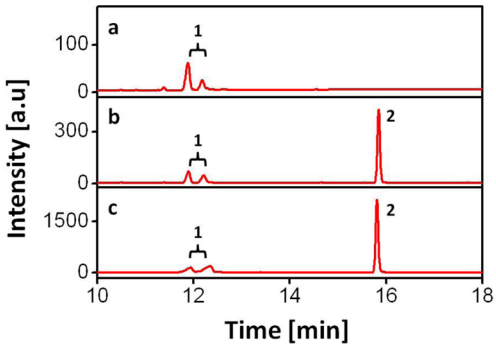

Figure 4. RP-HPLC analysis of **S1**, **S1-2**, and co-crystal **1·2**. (a,b) RP-HPLC analysis of 20 nm-thick **S1** and the corresponding **S1-2**. The chromatograms were obtained by dissolving the deposited organic materials in ACN:H_2O (v/v = 1:1). (c) RP-HPLC chromatogram of co-crystal **1·2** grown from solution. The co-crystal was redissolved in ACN:H_2O (v/v = 1:1) for analysis purposes. The peaks observed at retention times of 11.9 and 12.2 min correspond to compound **1**. Their relative intensities are concentration dependent, indicating the presence of aggregates (Figure S8).

To demonstrate the role of XB and the temperature in the conversion from **S1** to **S1-2**, we exposed **S1** to vapors of hexafluorobenzene (**3**; 120 °C, 18 h). Compound **3** is a poor XB donor.[28] No significant changes, compared to the UV/vis absorbance or XRD pattern of **S1**, were observed (Figure S10a,c). Compound **3** was not detected by HPLC analysis (Figure S11). AFM shows that heating **S1** (120 °C, 18 h) somewhat affects the shape of the grains (Figure S12b), and one of the XRD signals is slightly shifted compared to the unannealed **S1** (Figures S12c). However, these observations could not account for the morphology and crystallinity changes observed for **S1-2**. The observed crystal-to-co-crystal conversion (**S1** → **S1-2**) is mediated by XB, and the XB donor (**2**) is incorporated into the structure (**S1-2**) displaying characteristics similar to the co-crystal grown from solution. Mechanistically, the **S1** → **S1-2** conversion can occur through molecular diffusion involving surface migration and diffusion through the vapor phase.[29,30] Similar results were obtained when exposing the 50 nm-thick **S1** to vapors of compound **2** under the same conditions (Figures S4−S6 and S14−S15). However, a lower relative intensity was obtained for the XRD signal at 2θ = 5.75° after reacting the 50 nm-thick **S1** with **2** (Figure S6), compared to that obtained for the 20 nm-thick **S1** after reaction with **2** (Figure 3b). This effect suggests that the film thickness is a key parameter that determines the efficiency of the co-crystallization.

To explore the scope of our approach, we performed similar experiments using compound **4** as a different XB acceptor (Figure 1). This compound has three pyridyl units that may be involved in XB interactions with iodines in compound **2**.[21] **S4** and **S4-2** were obtained similarly to **S1** and **S1-2**, respectively. UV/vis spectroscopy measurements of **S4** displayed an absorption maximum at λ_{max} = 330 nm, indicating the deposition of compound **4** on the surface (Figure S2b).[27]

AFM measurements on silicon substrates revealed the formation of spherical islands (mean height = 33 ± 3 nm, surface coverage = 75%; Figures 2c and S16a,b). Examining the XRD pattern of **S4** revealed one single diffraction signal at 2θ = 24.98° corresponding to a spacing of d = 3.56 Å (Figure S17a). This value is within the range of $\pi-\pi$ stacking distances. Such a diffraction pattern may result from a turbostratic system.[31] The absence of the main intensity diffraction signals, compared to the powder diffraction pattern of compound **4** (Figure S17c), supports the formation of a non-crystalline material. UV/vis spectroscopy reveals slight broadening of the **S4-2** absorbance band compared to **S4** (Figure S18). In addition, the surface changes from spherical islands, observed for **S4**, to a fractal-like morphology for **S4-2** (Figures 2c,d and S16), suggesting a diffusion-limited aggregation process.[32] The presence of compound **2** in the resulting **S4-2** was confirmed by FD-MS (Table S1) and RP-HPLC (Figure S19), establishing its composite nature. However, no compelling evidence was found correlating the XRD pattern obtained for **S4-2** with the corresponding **4·2** co-crystal (Figure S17b,d). Control experiments with the poor XB donor **3** as well as thermal stability experiments with **S4** emphasize the role XB plays in directing the formation of **S4-2** (Figures S20−S21). These observations suggest that the initial crystalline nature of the XB-acceptor-functionalized surface (**S1** vs **S4**) can determine the feasibility of co-crystal formation; importantly, it does not inhibit the formation of a hybrid halogen-bonded system in **S4-2** composed of compounds **4** and **2**.

In conclusion, we have demonstrated an on-surface solvent-free crystal-to-co-crystal conversion. This conversion is achieved by exposing a surface-confined polycrystalline organic material to vapors of a complementary organic compound, yielding the corresponding co-crystal. The AFM images indicate that these transformations are accompanied by significant structural changes including formation of larger surface-bound structures. Therefore, molecular interpenetration is likely to be accompanied by a complex cascade of fusion processes. Our sequential solvent-free approach was demonstrated using XB as the driving force in the crystal-to-co-crystal conversion. Furthermore, we have shown that the scope of this approach is not limited to the formation of surface-confined co-crystals. Using a non-crystalline organic surface resulted in the formation of a halogen-bonded hybrid material with a different morphology. Our observations are in agreement with the findings by Metrangolo et al., who demonstrated that non-porous organic solids can dynamically resolve mixtures of diiodoperfluoroalkanes,[2a] indicating that a diverse range of systems might be available. Our presented system is mainly driven by XB interactions. PVD of single-component organics is known for the formation of other supramolecular materials based on hydrogen-bonding and $\pi-\pi$ stacking.[5] Moreover, the successful PVD of large molecules including polymers suggests that a large set of molecular systems might be used.[33] However, the use of PVD for the stepwise formation of multicomponent

dx.doi.org/10.1021/ja5066587 | J. Am. Chem. Soc. 2014, 136, 11926−11929

organic thin films is yet to be explored, as it might be a new entry for the formation of functional organic materials

■ ASSOCIATED CONTENT

Supporting Information

Experimental methods and more characterization data, AFM images, XRD patterns, TGA curves. This material is available free of charge via the Internet at http://pubs.acs.org.

■ AUTHOR INFORMATION

Corresponding Author

milko.vanderboom@weizmann.ac.il

Notes

The authors declare no competing financial interest.

■ ACKNOWLEDGMENTS

This research was supported by the Helen and Martin Kimmel Center for Molecular Design and the US-Israel Binational Science Foundation (BSF). Dr. Y. Feldman assisted with the XRD experiments (WIS). M.E.vdB. is the incumbent of the Bruce A. Pearlman Professorial Chair in Synthetic Organic Chemistry.

■ REFERENCES

(1) Desiraju, G. R. *J. Am. Chem. Soc.* **2013**, *135*, 9952−9967.

(2) (a) Metrangolo, P.; Carcenac, Y.; Lahtinen, M.; Pilati, T.; Rissanen, K.; Vij, A.; Resnati, G. *Science* **2009**, *323*, 1461−1464. (b) Pike, S. D.; Thompson, A. L.; Algarra, A. s. G.; Apperley, D. C.; Macgregor, S. A.; Weller, A. S. *Science* **2012**, *337*, 1648−1651. (c) van der Boom, M. E. *Angew. Chem., Int. Ed.* **2011**, *50*, 11846−11848. (d) Huang, Z.; White, P. S.; Brookhart, M. 2010, *465*, 598−601. (e) Inokuma, Y.; Kawano, M.; Fujita, M. 2011, *3*, 349−358. (f) Bezzu, C. G.; Helliwell, M.; Warren, J. E.; Allan, D. R.; McKeown, N. B. *Science* **2010**, *327*, 1627−1630. (g) Zenkina, O. V.; Keske, E. C.; Wang, R.; Crudden, C. M. *Angew. Chem., Int. Ed.* **2011**, *50*, 8100−8104.

(3) Zacher, D.; Schmid, R.; Wöll, C.; Fischer, R. A. *Angew. Chem., Int. Ed.* **2011**, *50*, 176−199.

(4) Ghorai, S.; Sumrak, J. C.; Hutchins, K. M.; Bucar, D.-K.; Tivanski, A. V.; MacGillivray, L. R. *Chem. Sci.* **2013**, *4*, 4304−4308.

(5) (a) Facchetti, A.; Annoni, E.; Beverina, L.; Morone, M.; Zhu, P.; Marks, T. J.; Pagani, G. A. *Nat. Mater.* **2004**, *3*, 910−917. (b) Lezama, I. G. r.; Nakano, M.; Minder, N. A.; Chen, Z.; Di Girolamo, F. V.; Facchetti, A.; Morpurgo, A. F. *Nat. Mater.* **2012**, *11*, 788−794. (c) DiBenedetto, S. A.; Frattarelli, D.; Ratner, M. A.; Facchetti, A.; Marks, T. J. *J. Am. Chem. Soc.* **2008**, *130*, 7528−7529. (d) Zhu, P.; Kang, H.; Facchetti, A.; Evmenenko, G.; Dutta, P.; Marks, T. J. *J. Am. Chem. Soc.* **2003**, *125*, 11496−11497.

(6) Blagden, N.; Berry, D. J.; Parkin, A.; Javed, H.; Ibrahim, A.; Gavan, P. T.; De Matos, L. L.; Seaton, C. C. *New J. Chem.* **2008**, *32*, 1659−1672.

(7) Yan, D.; Delori, A.; Lloyd, G. O.; Friščić, T.; Day, G. M.; Jones, W.; Lu, J.; Wei, M.; Evans, D. G.; Duan, X. *Angew. Chem., Int. Ed.* **2011**, *50*, 12483−12486.

(8) Chen, Q.; Chen, T.; Wang, D.; Liu, H.-B.; Li, Y.-L.; Wan, L.-J. P. *Natl. Acad. Sci. USA* **2010**, *107*, 2769−2774.

(9) Bruck, S.; Krause, C.; Turrisi, R.; Beverina, L.; Wilken, S.; Saak, W.; Lutzen, A.; Borchert, H.; Schiek, M.; Parisi, J. *Phys. Chem. Chem. Phys.* **2014**, *16*, 1067−1077.

(10) Duong, A.; Dubois, M.-A.; Maris, T.; Metivaud, V.; Yi, J.-H.; Nanci, A.; Rochefort, A.; Wuest, J. D. *J. Phys. Chem. C* **2011**, *115*, 12908−12919.

(11) Salammal, S. T.; Balandier, J.-Y.; Kumar, S.; Goormaghtigh, E.; Geerts, Y. H. *Cryst. Growth Des.* **2013**, *14*, 339−349.

(12) Braga, D.; Grepioni, F. *Chem. Commun.* **2005**, 3635−3645.

(13) Hassel, O.; Stromme, K. O. *Nature* **1958**, *182*, 1155−1156.

(14) Rabinovich, D.; Schmidt, G. M. J.; Shaked, Z. *J. Chem. Soc. B* **1970**, 17−24.

(15) Priimagi, A.; Cavallo, G.; Metrangolo, P.; Resnati, G. *Acc. Chem. Res.* **2013**, *46*, 2686−2695.

(16) Hardegger, L. A.; Kuhn, B.; Spinnler, B.; Anselm, L.; Ecabert, R.; Stihle, M.; Gsell, B.; Thoma, R.; Diez, J.; Benz, J.; Plancher, J.-M.; Hartmann, G.; Banner, D. W.; Haap, W.; Diederich, F. *Angew. Chem., Int. Ed.* **2011**, *50*, 314−318.

(17) Ren, J.; He, Y.; Chen, W.; Chen, T.; Wang, G.; Wang, Z.; Xu, Z.; Luo, X.; Zhu, W.; Jiang, H.; Shen, J.; Xu, Y. *J. Med. Chem.* **2014**, *57*, 3588−3593.

(18) Bolton, O.; Lee, K.; Kim, H.-J.; Lin, K. Y.; Kim, J. *Nat. Chem.* **2011**, *3*, 205−210.

(19) Meazza, L.; Foster, J. A.; Fucke, K.; Metrangolo, P.; Resnati, G.; Steed, J. W. *Nat. Chem.* **2013**, *5*, 42−47.

(20) Lucassen, A. C. B.; Zubkov, T.; Shimon, L. J. W.; van der Boom, M. E. *CrystEngComm* **2007**, *9*, 538−540.

(21) Vartanian, M.; Lucassen, A. C. B.; Shimon, L. J. W.; van der Boom, M. E. *Cryst. Growth Des.* **2008**, *8*, 786−790.

(22) Lucassen, A. C. B.; Karton, A.; Leitus, G.; Shimon, L. J. W.; Martin, J. M. L.; van der Boom, M. E. *Cryst. Growth Des.* **2007**, *7*, 386−392.

(23) Priimagi, A.; Saccone, M.; Cavallo, G.; Shishido, A.; Pilati, T.; Metrangolo, P.; Resnati, G. *Adv. Mater.* **2012**, *24*, OP345−OP352.

(24) Shirman, T.; Freeman, D.; Posner, Y. D.; Feldman, I.; Facchetti, A.; van der Boom, M. E. *J. Am. Chem. Soc.* **2008**, *130*, 8162−8163.

(25) Shirman, T.; Kaminker, R.; Freeman, D.; van der Boom, M. E. *ACS Nano* **2011**, *5*, 6553−6563.

(26) Clarke, S. M.; Friščić, T.; Jones, W.; Mandal, A.; Sun, C.; Parker, J. E. *Chem. Commun.* **2011**, *47*, 2526−2528.

(27) Shukla, A. D.; Strawser, D.; Lucassen, A. C. B.; Freeman, D.; Cohen, H.; Jose, D. A.; Das, A.; Evmenenko, G.; Dutta, P.; van der Boom, M. E. *J. Phys. Chem. B* **2004**, *108*, 17505−17511.

(28) Politzer, P.; Murray, J. S.; Clark, T. *Phys. Chem. Chem. Phys.* **2010**, *12*, 7748−7757.

(29) Rastogi, R. P.; Bassi, P. S.; Chadha, S. L. *J. Phys. Chem.* **1963**, *67*, 2569−2573.

(30) Friščić, T.; Jones, W. *Cryst. Growth Des.* **2009**, *9*, 1621−1637.

(31) Yang, D.; Frindt, R. F. *J. Mater. Res.* **1996**, *11*, 1733−1738.

(32) Witten, T. A., Jr.; Sander, L. M. *Phys. Rev. Lett.* **1981**, *41*, 1400−1403.

(33) Li, L.; Li, B.; Yang, G.; Li, C. Y. *Langmuir* **2007**, *23*, 8522−8525.